International Conference on Applied Energy 2019
Aug 12-15, 2019, Västerås, Sweden
Paper ID: #242

WETTABILITY OF [BMIM] [BF_4] IONIC LIQUID DROPLET ON HYDROPHOBIC AND HYDROPHILIC SUBSTRATES

Fenhong Song, Bing Ma, Jing Fan, Gang Wang, Tieliu Jiang*
School of Energy and Power Engineering, Northeast Electric Power University, Jilin, Jilin 132012, China.

ABSTRACT
In this paper, molecular dynamics method was employed to investigate the wetting and electro-wetting behaviors of nano-droplet of ionic liquid on a solid substrate with different wettability. The results show that the anion and cation groups are distributed in layers above the wall. The static contact angle decreases obviously when epsilon increases from 0.1 to 0.6 On the hydrophobic surface (ε=0.1), the droplet shows an asymmetric wetting when the imposed vertical electric field is in positive and negative direction. While on the hydrophilic surface (ε=3.0), the wetting of ILs droplet becomes nearly asymmetric because the strong solid attraction tend to dominate the wetting process. Through analyzing the distribution of coarse particles, it's found that the asymmetric wetting is caused by the fact that the diffusion of cations on the substrate surface is stronger than that of anions.

Keywords: electro-wetting, ILs droplet, asymmetric wetting, molecular simulation.

1. INTRODUCTION

As an advanced and efficient microfluidic driving technology, electro-wetting driven by electric field are of great interest in microcomputer electrical systems such as supercapacitor, electronic paper, transistor, lab-on chip, and microzoom lens[1-3]. Compared with saline solution, Ionic liquid (IL) has attracted wide attention in the field of wetting and electro-wetting due to their good conductivity, long liquid length and low volatility.

The wetting of IL under free diffusion is mainly affected by ion species, electrostatic forces between anions and anions, adsorption force of solid substrate and microstructures of solid surface. The contact angle decreases with the adsorption force of substrate[4, 5] and increases with the number of ions[4]. The compatibility of IL with different microstructures of surface is different[4, 6, 7], Castejón[6] studied the wettability of five types of ILs on solid substrates with different microstructures, and found that the contact angles of four types of ILs on the surface coated with hydroxyl groups (Si-OH) are smaller than those on the surface coated with hydrogen groups (Si-H).

Compared with wetting, the influence of electric field on the wettability of IL is mainly reflected in electric field strength[8] and electric field direction[5, 9]. The contact angle of IL decreases with the increase of field strength, as does the traditional saline solution[10, 11]. Compared with the asymmetry phenomenon under the positive and negative field with weak strength[9], the asymmetry phenomenon of the droplet induced by the field with strong strength is more obvious, including experiment[12-14] and simulation[15]. Dong[5] simulates the [EMIM][TFSI] droplet wetting on a single graphene under positive and negative field, and found that the difference of contact angle is 6.6° at E=±0.136 V/Å. Liu[9] found that the droplet is more likely to diffuse on the substrate under the negative field, and the contact angle is smaller than that under the positive field. However, the micro-mechanism of asymmetric wetting is unclear up to now. In this paper, 1-Butyl-3-methyl tetra-fluoroborate ([BMIM][BF_4]) droplet and coarse-grained model is selected to study wetting characteristics of IL droplet on substrate and the distribution of coarse particles to analyze the micro-mechanism of asymmetric wetting.

2. SIMULATION DETAILS

2.1 Simulation model

The molecular dynamics model of IL droplets wetting on solid substrate is shown in fig 1. The solid substrate is composed of 12544 silicon atoms arranged in a cubic crystal structure with a size of 170 × 9.5 × 170 $Å^3$. A spherical droplet containing 500 pairs of

Selection and peer-review under responsibility of the scientific committee of the 11th Int. Conf. on Applied Energy (ICAE2019).

[BMIM][BF_4] ILs. The molecular formula and structure corresponding to the cation and anion of [BMIM][BF_4] are given in fig 1. The coarse-grained model developed by Merlet[16] is used to simplify the simulation, in which C1, C2, C3 and A coarse particles represent the imidazolium ring, ethyl group and alkyl tail, and the whole anion, respectively. The relative positions of the three coarse particles in the cation are fixed to construct a rigid body that can be rotated and translated freely. The mass of each coarse particle is the sum of the masses of all including atoms, and the center of each coarse particle is the center of mass. The length of C1C2 and C1C3 bonds are 2.7 Å and 3.8 Å，and the C3C1C2 angle is 106°. In previous study, it has been verified that the results calculated from coarse-grained model is consistent well with the all-atom force field[15]. Therefore, the coarse-grained model is widely used in molecular simulations of IL due to its simple form and high accuracy.

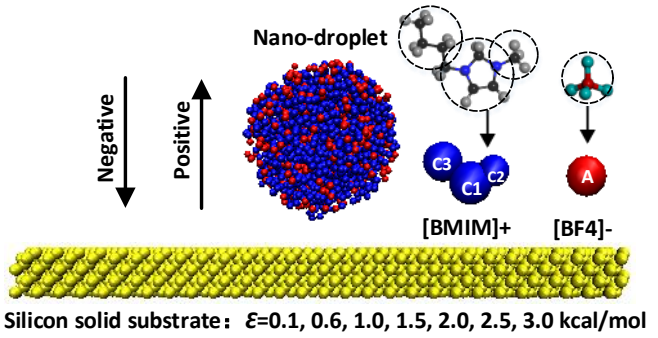

Fig 1 Wetting Model of Nanoparticle on solid substrate and Coarse-particle Model of IL (C1: Cationic Ring, C2: Methyl Chain, C3: Butyl Chain, A: Anion)

The forces between the anionic and cationic coarse particle groups of IL are composed of short range Van der Waals' forces and long range Coulombic interactions, which are calculated by the classic Lennard-Johns (L-J) potential function and Coulomb law as follows,

$$U_{ij}=\frac{q_i q_j}{r_{ij}}+4\varepsilon_{ij}\left[\left(\frac{\sigma_{ij}}{r_{ij}}\right)^{12}-\left(\frac{\sigma_{ij}}{r_{ij}}\right)^{6}\right] \quad (1)$$

Where q_i, q_j are the charges on coarse particle *i* and *j*, σij, εij represent the scale and energy parameters, respectively. The interactions between the coarse particles and the atoms on solid substrate are characterized by the modified L-J potential function, and the corresponding scale and energy parameters are obtained by Lorentz-Berthelot mixing rules. Table 1 gives the parameters of each coarse particle and silicon atoms.

Molecular dynamics simulations are carried out using the Lammps package under NVT ensemble. The Nose-Hoover thermostat is used to control the temperature constant at 298 K and the Velocity-verlet algorithm is chosen to solve the equation of motion. The particle−particle-particle−mesh (PPPM) method[17] is used to calculate the long-range coulombic interactions, and the cutoff radius of 15 Å is applied to short-range Van der Waals' forces and electrostatic calculations. The time step is set to be 2 fs. The droplets wet seven substrates freely with different energy parameters (ε=0.1, 0.6, 1.0, 1.5，2.0, 2.5, 3.0 kcal/mol) and reaches a static state in the absence of electric field in 10 ns. Then electric fields of E=±0.08 V/Å and E= ±0.18 V/Å in the vertical direction are applied to the droplets to investigate to its electro-wetting behaviors on silicon substrate.

Table 1 Parameters of coarse particles and Si atoms

Group	M (g/mol)	ε (kcal/mol)	σ (Å)	q (e)
C1	67.07	0.6116	4.38	0.4374
C2	15.04	0.0860	3.41	0.1578
C3	57.12	0.4372	5.04	0.1848
A	86.81	0.7740	4.51	-0.7800
Si	28.08	0.1, 0.6, 1.0, 1.5, 2.0, 2.5, 3.0	3.39	0.0000

2.2 Calculation of contact angle

When the IL droplets diffuse to an equilibrium state on the substrate, the contact angle is obtained by making a two-dimensional ion number density contour[12,13]. In this paper, the simulation box is divided into 75 × 75 × 75 small cubes, and the side length of each small cube is 2 Å, and then the number of particles(C1, C2, C3 and A) in each cube is calculated. The total mass of particles in each small cube is obtained by multiplying the number of cationic and anionic particles by their respective masses, and the number density in the cube [12,13] is improved to the mass density to obtain the calculation method of contact angle.

3. SIMULATION DETAILS

3.1 Free diffusion of IL droplets on hydrophilic and hydrophobic substrate

In this section, the free diffusion of IL droplets on the solid substrates with different energy parameters is simulated. The free diffusion of IL droplets on the substrate is shown in fig 2. It is found that the contact angle decreases with the increase of ε in a range of low strength ε. While it decrease very slightly with the

further increase of ε when $\varepsilon \geq 2.0$. *E. g.* The static contact angles of ILs droplet on solid surface with ε=0.1, 0.6, 2.5 and 3.0 are 115°, 86°, 65° and 64°, respectively.

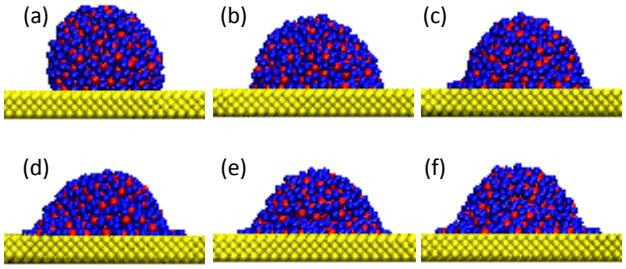

Fig 2 The diffusion of droplets on substrates with different ε. (a) ε=0.1 kcal/mol; (b) ε=0.6 kcal/mol; (c) ε=1.0 kcal/mol; (d)ε=2.0 kcal/mol; (e) ε=2.5 kcal/mol; (f) ε=3.0 kcal/mol

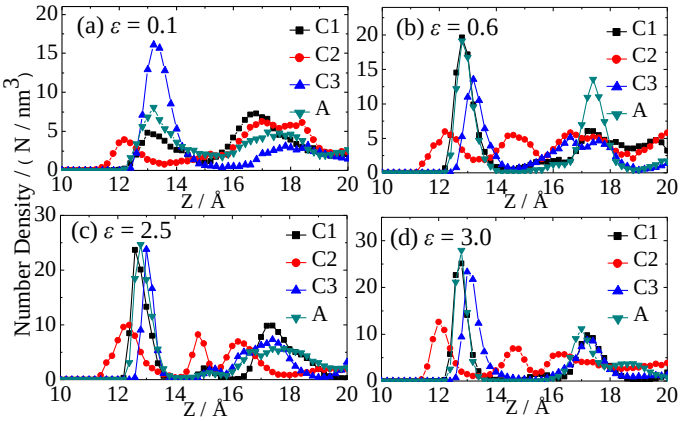

Fig 3 The number density for C1, C2, C3 and A under different ε

In order to further discuss the reason that the diffusion characteristics and contact angles on the substrate change indistinctly at high strength ε, the distributions of particles' number density with height on the substrate with different ε are given, as shown in fig 3. In these cases, the distributions of the number density of cations and anions in the first wetting layer (10 Å-15 Å) close to the substrate reflect the adsorption capacity of the substrate to the droplets. When ε increases from 0.1 kcal/mol to 0.6 kcal/mol, the peak values of the number density of C1 and A increase rapidly in the first layer, while the peak values do not change significantly when ε increases from 2.5 kcal/mol to 3.0 kcal/mol. When ε=0.1~0.6 kcal/mol, the distributions of coarse particles in the first wetting layer are loose and the number density is small see Fig.3 (a-b)). With the increase of ε, more coarse particles are adsorbed to the first wetting layer by the substrate, resulting in the increase of the peak values. When ε=2.5~3.0 kcal/mol, the distributions of coarse particles in the first wetting layer are tight with a large number density (see Fig.3 (c-d)). With the increase of ε, the first wetting layer with saturated number density cannot accommodate more coarse particles, so the number density of the first wetting layer will hardly increase with the increase of ε and the wetting contact angle is almost the same. Therefore, analyzing the distributions of coarse particles in the first wetting layer close to the substrate is an effective way to analyze the wetting characteristics of droplets.

3.2 Diffusion induced by electric fields

To investigate the electro-wetting behavior of ILs droplet, the electric fields of E=±0.08 V/Å and E=±0.18 V/Å are applied to the system after the droplet reach to a static state in the absence of electric field. Fig 4 shows the mass density profile of the droplets under positive and negative electric fields when ε=0.1, 0.6 and 2.0 kcal/mol. And the corresponding contact angle is given in fig 5.

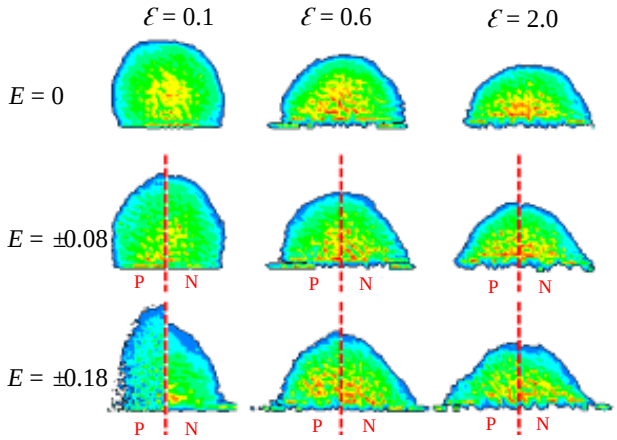

Fig 4 Diffusion induced by electric fields. The left is the positive fields; the right is the negative fields

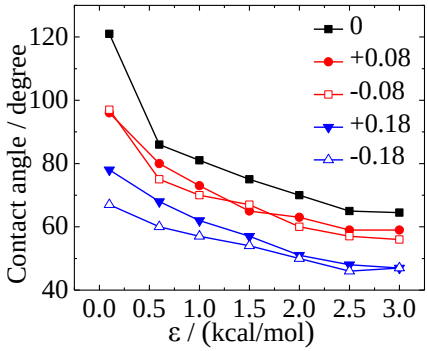

Fig 5 The change of contact angles with positive and negative electric fields at different strength of ε

In fig 4, the droplets on the solid surface with ε=0.1, 0.6 and 2.0 kcal/mol spread laterally with the increase of electric fields, and their contact angles decrease with the increase of electric fields, as shown in fig 5. When ε=0.1 kcal/mol and E=-0.18 V/Å, the contact angle of droplet decreases from 121° to 67°, and the range of

change is 54°, compared with free diffusion; When ε=3.0 kcal/mol and E=-0.18 V/Å, the contact angle of droplet decreases from 64.5° to 47°, and the range of change is 17.5°, compared with free diffusion. Compared with the range of high strength ε, the adsorption force of substrate on the droplets is small, and the applied electric field dominates the change of diffusion and contact angle, and the change of electric field is more likely to affect the wetting characteristics of the droplets at the range of low strength ε.

Moreover, fig 4 also reflects the asymmetry of diffusion and contact angles under positive and negative electric fields. In most working conditions, the contact angles of droplets under negative direction are slightly lower than that under positive direction. Especially at ε=0.1 kcal/mol, E=±0.18 V/Å, $\theta_{postive} < \theta_{negative}$, the angle difference is about 10°. $H_{positive} > H_{negative}$, the height difference is about 15 Å. Compared with the condition ε=0.1 kcal/mol, E=+0.18 V/Å, at ε=0.1 kcal/mol, E=-0.18 V/Å, cationic particles in the first wetting layer are closer to the surface of substrate, and the ability of cations to diffuse on the surface of substrate is greater than that of anions, resulting in the asymmetry of the contact angles.

In order to verify the asymmetry due to the fact that the diffusion of cations on the surface of substrate is stronger than that of anions, the number density of cationic and anionic particles under the condition of ε=0.1 kcal/mol, E=±0.18 V/Å is depicted here, as shown in fig 6 (a) (b). The number density under the condition of ε=2.0 kcal/mol, E=±0.18 V/Å with no obvious asymmetry is also given, as shown in fig 6 (c) (d) to compare with fig 6 (a) (b).

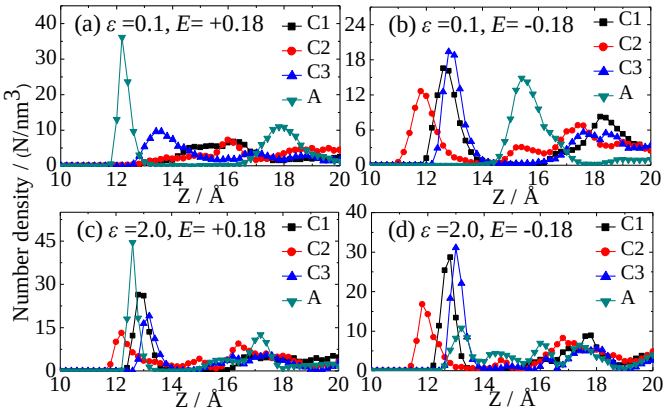

Fig 6 The number density of cationic and anionic particles

Under the positive electric field in fig 6 (a), the peak values of cations in the first wetting layer are all less than 10/nm^3, and the peak positions are not obvious. Under the negative electric field shown in fig 6 (b), the peak values of cations in the first wetting layer move forward and the peak heights increase significantly. Cations accumulate in the first wetting layer and diffuse on the surface of substrate, which also explains the asymmetry under the condition of ε=0.1 kcal/mol, E=±0.18 V/Å.

However, anions in the droplet have no obvious effects on asymmetric wetting. As shown in fig 6 (c) and 6 (d), the peaks of C1 and C3 fluctuate between 20/nm^3 and 30/nm^3. Though the peak value of anions decreases from 45/nm^3 to 10/nm^3, the droplet still has a nearly symmetric wetting on the solid surface with epsilon equals to 2.0. This indicates that the accumulation of anions in the first wetting layer and the diffusion of anions on the surface of substrate do not cause asymmetric wetting under the condition of ε=2.0 kcal/mol, E=±0.18 V/Å.

4. CONCLUSIONS

In this paper, molecular dynamics method was employed to investigate the wetting and electro-wetting (E=±0.08 V/Å and E=±0.18 V/Å) behaviors of IL nano-droplets on a solid substrate with different energy parameters epsilon changing from (from ε=0.1 kcal/mol to ε=3.0 kcal/mol), as well as the distribution of ionic groups. Compared with the weak adsorption force of substrate where ε=0.1 kcal/mol, the cationic and anionic particles in the first wetting layer are tightly arranged and spread over a wide range on the substrate with strong adsorption where ε=3.0 kcal/mol. When applying electric field on the system, the ILs droplet shows an asymmetric wetting under electric field in positive and negative direction. The asymmetry of the droplets on the substrate with lower epsilon is more obvious than that on the substrate with strong adsorption force. Through analyzing the distribution of cationic and anionic particles, it has been found that asymmetric wetting is determined by the diffusion of cations in the first wetting layer.

ACKNOWLEDGEMENT

The authors would like to acknowledge the support from the National Natural Science Foundation of China (Grant No.51606032)

REFERENCE

[1] Vatamanu J, Vatamanu M, Bedrov D. Non-faradaic energy storage by room temperature ionic liquids in nanoporous electrodes. ACS Nano 2015; 9: 5999-6017.

[2] Wang F, Stepanov P, Gray M, et al. Ionic liquid gating of suspended MoS\r, 2\r, field effect

transistor devices[J]. Nano Lett. 2015; 15: 5284-5288.
[3] Peng RL, Chen JB, Zhu C. Design of a zoom lens without motorized optical elements. Opt. Express 2007; 15: 6664-6669.
[4] Herrera C, Garcia G, Atilhan M, et al. Nanowetting of graphene by ionic liquid droplets. J. Phys. Chem. C 2015; 119: 24529-24537.
[5] Dong DP, Vatamanu J, Bedrov D, et al. The 1-Ethyl-3-Methylimidazolium Bis(Trifluoro-Methylsulfonyl)-Imide ionic liquid nanodroplets on solid surface and in electric field: A molecular dynamics simulation study. J. Chem. Phys. 2018; 148: 193833-193841.
[6] Castejón HJ, Wynn TJ, Marcin ZM. Wetting and tribological properties of ionic liquids. J. Phys. Chem. B 2014; 118: 3661-3668.
[7] Liu J, Li J, Yu B, et al. Tribological properties of self-assembled monolayers of catecholic imidazolium and the spin-coated films of ionic liquids. Langmuir 2011; 27: 11324-11331.
[8] Restolho J, Mata JL, Saramago B. Electrowetting of ionic liquids: contact angle saturation and irreversibility. J. Phys. Chem. C 2009; 113: 9321-9327.
[9] Liu Z, Cui T, Li GZ, et al. Interfacial nanostructure and asymmetric electrowetting of ionic liquids. Langmuir 2017; 33: 9539-9547.
[10] Song FH, Li BQ, Li Y, et al. Dynamic spreading of a nanosized droplet on a solid in an electric field. Phys. Chem. Chem. Phys. 2015, 17(8): 5543-5546.
[11] Ren H, Zhang L, Li X, et al. Interfacial Structure and Wetting Properties of Water Droplets on Graphene under a Static Electric Field. Phys. Chem. Chem. Phys. 2015; 17: 23460-23467.
[12] Gamerocastano M. Electric-field-induced ion evaporation from dielectric liquid. Phys. Rev. Lett. 2002; 89: 147602.
[13] Paneru M, Priest C, Sedev R, et al. Static and dynamic electrowetting of an ionic liquid in a solid/liquid/liquid system. J. Amer. Chem. Soc. 2010; 132: 8301-8308.
[14] Millefiorini S, Tkaczyk AH, Sedev R, et al. Electrowetting of ionic liquids. J. Amer. Chem. Soc. 2006; 128: 3098-3101.
[15] Taherian F, Leroy F, Heim LO, et al. Mechanism for asymmetric nanoscale electrowetting of an ionic liquid on graphene. Langmuir 2015; 32: 140-150.
[16] Merlet C, Salanne M, Rotenberg B. New coarse-grained models of imidazolium ionic liquids for bulk and interfacial molecular simulations. J. Phys. Chem. C 2013; 116: 7687-7693.
[17] Beckers JVL, Lowe CP, De Leeuw S W. An iterative PPPM method for simulating coulombic systems on distributed memory parallel computers. Mol Simulat 1998; 20: 369-383.